한국동력기계공학회지 제16권 제2호 pp.36~42 2012년 4월

Pellet Geometric Effects on a Thermoelectric Generator with a High Power Electronic Component
고파워 전자소자에 부착된 열전생성기에 대한 pellet의 기학학적 구조가 미치는 영향

K. J. Kim
김 경 준

(received 07 December 2011, revised 02 February 2102, accepted 15 February 2012)

Key Words : 열전(Thermoelectric), 열전생성기(Thermoelectric Generator), 에너지수확(Energy Harvesting)

Abstract : 본 논문은 고파워 전자소자로부터 에너지를 수확하는 열전생성기의 성능에 pellet의 기학학적 구조가 미치는 영향들을 보고한다. 열경계저항을 포함하는 열전모델을 적용하여, 다양한 경계조건들과 열원의 열율들에 대해 pellet의 높이, pellet의 단면적, thermocouple의 수를 최적화 하고, 이처럼 최적화된 pellet의 기하학적 구조를 갖는 열전생성기의 성능과 일반적인 pellet으로 구성된 열전생성기의 전력생성성능과 효율이 예측되고 비교되어진다. 예측된 결과는 최적화된 pellet으로 구성된 열전생성기가 일반적인 pellet으로 구성된 열전생성기보다 2-10배까지 생성효율이 우수함을 보여준다. 최적화된 pellet으로 구성된 열전생성기와 일반적인 pellet으로 구성된 열전생성기의 열적성능도 예측되고 비교된다.

1. 서 론

Electronic components waste tremendous amount of heat, eventually dissipated to the environment. For example contemporary power amplifier transistors of base stations dissipate nearly 30% of the total energy consumed by a wireless access network to the environment. Hence, the waste heat of electronics can be useful energy if the effective energy harvesting technique is established.

Thermoelectric generators (TEGs) have been used to build power generating systems to provide electricity in harsh or remote environments since 1960s[1]. Major applications are to power telecommunication equipment and to protect metal corrosion in remote area. TE power generating systems contain heaters providing TEGs with thermal energy. Heaters use either fossil fuels or radioisotopes. Despite the intensive use of TEGs as sub-modules for power generation, TEGs have been recently considered as potential energy harvesters from waste heat. There are recently reported researches such as TE power generation from CPU waste heat[2-3], Si-Ge based TEGs applied to gasoline engine vehicles, bismuth telluride based TEGs applied to diesel engines[4], TE power generation systems applied to generate the electricity from municipal waste heat[5], and a TE power generator using solar heating, etc.

Nanostructure-based TE materials have been reported to have higher figure of merits (FOMs) than classical TE materials[6-7]. Nevertheless, technical difficulties in fabricating, packaging, and scaling prevent the use of such advanced TE materials for real applications. The right methodology improving TEGs performance in the system level can be an alternative solution to enhance energy harvesting performance from high power components[8]. Optimized pellet geometries can be a good solution to improve the

K. J. Kim(corresponding author) : Department of Mechanical & Automotive Engineering, Pukyong National University.
E-mail: kjkim@pknu.ac.kr, Tel: 051-629-6168

system-level performance of the TEG. However, any published reports do not show the prediction methodology or the behavior of the TEG performance associated with optimized pellet geometries to harvest the energy from high power electronic components. Hence, this paper is aimed at providing the prediction methodology of the TEG performance associated with optimized pellet geometries and the effect of the optimized pellet geometries on the power generating and the thermal performances of the TEG.

In methodology sections this paper provides a thermoelectric model containing thermal boundary resistances and the measurement method of the TEG performance. In result sections first, this paper provides determined optimized pellet geometries. Secondly, the paper discusses comparative study results between the TEG associated with optimized pellet geometries and the TEG with conventional pellet geometries regarding the power generating performance, the generation efficiency, the thermal performance of the TEG for various thermal interfacial conditions at various source heat rates.

2. Thermoelectric model

Basic physics of thermoelectric energy conversion with a thermocouple is illustrated in Fig. 1. The thermocouple contains p-type and n-type semiconductors, interconnects, and insulation layers. Pellets, i.e., semiconductor columns, are electrically in series and thermally in parallel. A few hundreds of thermocouples generate a thermoelectric generator (TEG).

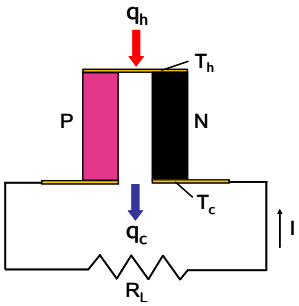

Fig. 1 A thermocouple in power generation mode

A heat rate to the hot side, q_h, creates a temperature difference across the thermocouple, i.e., T_h-T_c where T_h and T_c are hot and cold side temperatures, respectively. Due to Seebeck and Peltier effects, an electrical current, I, is generated via the load resistor, R_L, in a closed circuit.

The current, I, is defined in a fractional form as

$$I = \frac{N\alpha(T_h - T_c)}{NR + R_L} \tag{1}$$

where N is the number of thermocouples, a is a Seebeck coefficient, and R is the electrical resistance of the thermocouple.

The numerator, $Na(Th-Tc)$, is the voltage generated across the TEG. The denominator, $NR+RL$, is the electrical resistance of the generation system.

R is defined as:

$$R = \frac{2\rho H}{A_p} + R_c \tag{2}$$

where ρ is the electrical resistivity of the pellet, H is a pellet height, Ap is a pellet cross sectional area, and Rc is the electrical contact resistance of a thermocouple. Rc is defined as $4Rc-\rho/Ap$ where $Rc-\rho$ is an electrical contact resistivity.

qh and qc are defined[1] as

$$q_h = NI\alpha T_h + (T_h - T_c)/\psi_{TEG} - NI^2R/2 \tag{3}$$

$$q_c = NI\alpha T_c + (T_h - T_c)/\psi_{TEG} + NI^2R/2 \tag{4}$$

where qc is the heat rate out of the cold side, and ΨTEG is the TEG thermal resistance.

Physical significance is embedded in terms of Eqs. (3) and (4). $NIaTh$ and $NIaTc$ are the energy terms due to the Peltier effect.

$(Th-Tc)/\psi TEG$ is the heat conduction purely induced by a temperature difference across pellets. $NI^2R/2$ shows the Joule heating effect.

ΨTEG is defined as:

$$\psi_{TEG} = \frac{H}{2NkA_p} \tag{5}$$

where k is the thermal conductivity of the pellet. The generated power, P_L, is defined as

$$P_L = I^2 R_L \tag{6}$$

The energy balance for the TEG shows that q_c is the remained amount of the energy after subtracting the generated power, P_L, from q_h.

The generation efficiency (thermodynamic efficiency) is defined as

$$\eta = P_L / q \tag{7}$$

Fig. 2 shows the proposed structure of a thermoelectric energy harvesting module to recover the energy from the waste heat of a heat source, i.e., a high power electronic component. A heat spreader is used to reduce the thermal resistance between a heat source and the TEG. A heat sink is placed to effectively dissipate the waste heat of the heat source to the ambient. Thermal interface materials (TIMs) are applied on the interface between a component and the heat spreader and on the interfaces between hot and cold sides of the TEG and the heat spreader and the heat sink.

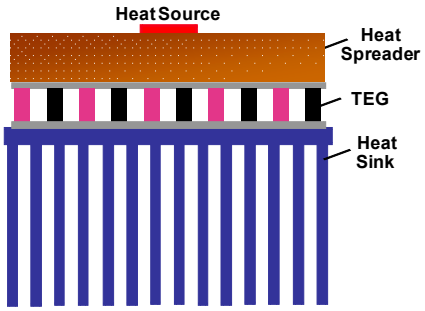

Fig. 2 Structure of a thermoelectric energy harvesting module

Fig. 3 shows the illustrated physical structure of the TEG model associated with a high power component. The model concatenates thermoelectricity and heat transfer. q is the total heat rate from the source, and q_c is the heat rate out of the cold side of the TEG, denoted by the subscript c. The subscripts j and a denote the junction and the ambient. Ψ_{jh} and Ψ_{ca} are thermal resistances between j and h and between c and a. It should be noted that a generation cycle is embedded in a thermal network.

Assuming negligible convective heat loss compared with the heat conducted from j to h, q can be considered to be equal to qh.

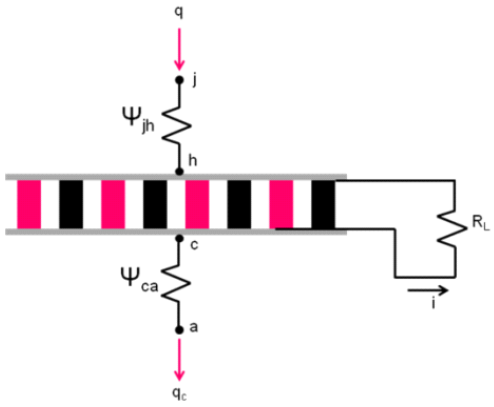

Fig. 3 Physical structure of a TEG model

Hence, q can be expressed as

$$q = (T_j - T_h)/\psi_{jh} \tag{8}$$

where Tj is the junction temperature.

qc can be expressed as

$$q_c = (T_c - T_a)/\psi_{ca} \tag{9}$$

where Ta is the ambient temperature.

Following equations are generated by incorporating (3) with (8) and (4) with (9)

$$q = NI\alpha T_h + (T_h - T_c)/\psi_{TEG} - NI^2R/2 = (T_j - T_h)/\psi_{jh} \tag{10}$$

$$q_c = NI\alpha T_c + (T_h - T_c)/\psi_{TEG} + NI^2R/2 = (T_c - T_a)/\psi_{ca} \tag{11}$$

Solving Eqs. (1,2), (5,6), and (10,11) simultaneously, one may predict both the power generation and the thermal performance of the TEG associated with an electronic component.

3. Measurement method

The experimental setup has been constructed to measure generated powers and junction temperatures of the thermoelectric energy

harvesting module. A generated test vehicle contains a TEG, a heat source, a heat spreader, and a heat sink. To generate the test vehicle, a Marlow TEG (TG 12-2.5) having the footprint of 30mm×34mm has been used. Number of thermocouples is 127, pellet height is 1.78mm, and pellet cross sectional area is 0.98 mm^2. The copper heat spreader has been used to reduce the spreading resistance between the source and the TEG hot side. The heat spreader is 50mm wide, 50mm long, and 10mm thick.

A heat sink has been used to effectively dissipate the heat rate from the TEG cold side to the ambient. The used heat sink is a 60mm wide and 57mm long aluminium plate fin heat sink. Fin height, number of fins, and fin thickness are 34mm, 20, and 1mm, respectively. The heat sink resistance associated with an air velocity of 2m/s was 0.5K/W.

A utilized 8mm × 8mm ceramic heater simulates a high power electronic component, e.g. a power amplifier transistor. The heater has been attached on the heat spreader top surface applying a thermal epoxy with a thermal conductivity of 1W/m-K. The TEG has been packaged between the heat spreader and the heat sink utilizing thermal adhesive tapes.

An experimental setup is shown in Fig. 4. Both air flow rate and air flow profile are needed to be controlled to provide proper aerodynamic conditions for the heat sink, and thus a portable wind tunnel (120mm ×120mm × 400mm) has been constructed. 10mm thick plexy glass sheets have constructed windows. An axial fan (Ebm-papst 4118NHH), implemented in the outlet of the wind tunnel, provides the air flow to the heat sink. A 50mm thick honeycomb, implemented in the wind tunnel inlet, enables the uniformity of the air flow.

The test vehicle has been placed on the open section of the top window of the wind tunnel. Two supporting bars and auxiliary units mechanically support the test vehicle. An insulation sheet (Aspen aerogel) has insulated the exposed surface of the heat spreader. A pitostatic tube and a micromanometer (FCO010) have monitored an incident air velocity to the heat sink. A data logger (Agilent 34970A) associated with K-type thermocouples and a data acquisition PC have monitored temperatures at the heater, the heat sink base, and the ambient.

The power generation circuit contains a shunt resistor and a load resistor as shown in Figure 4. A 1mΩ current sense resistor is used as a shunt resistor. The current through the circuit is determined by applying Ohms' law for a measured DC voltage across the shunt resistor.

A potentiometer is used as a load resistor, and the DC voltage across the load resistor is measured. Multiplying the voltage across the load resistor by the current determines the value of the generated power. The further information with respect to the measurement setup can be found in a published report[9].

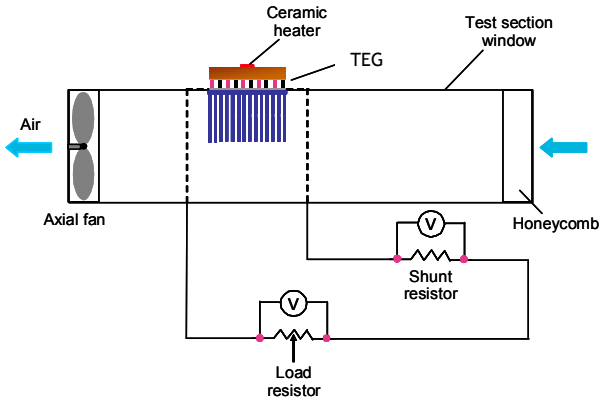

Fig. 4 Schematic of measurement setup

4. TEG performances

This section provides optimized pellet geometries, power generating and thermal performances of TEGs with optimized pellet geometries and with conventional pellet geometries at various source heat rates for two interfacial conditions.

4.1 Prediction and Measurement Conditions of the TEG

Tables 1 summarizes prediction and measurement

conditions of TEGs. Case I is a predicted case with optimized pellet geometries and ideal interfaces with no interfacial resistances. Ψ_{jh} of 0.13 and Ψ_{ca} of 0.5 are used for the case I. Case II is a predicted case with optimized pellet geometries and 5 mil (127μm) thick interfaces. The interfaces are TIMs with a thermal conductivity of 0.8W/m-K. Ψ_{jh} of 2.8 and Ψ_{ca} of 0.7 are used for the case II. Case III and IV are predicted cases with actual pellet geometries of a commercially available TEG and no interfacial resistance condition (case III) and 5 mil interface condition (case IV). The TEG used for the measurement has same pellet geometries compared with cases III and IV. Pellet height is 1.78mm, pellet cross sectional area is 0.98mm^2, and number of thermocouples is 127 for the cases III and IV and the measurement.

Table 1: Prediction and measurement conditions

Case	Pellet geometries	ψ_{jh} (K/W)	ψ_{ca} (K/W)	Interface
I	optimized	0.13	0.5	no resistance
II	optimized	2.8	0.7	5 mil thick
III	off-the-self	0.13	0.5	no resistance
IV	off-the-self	2.8	0.7	5 mil thick
Measur-ement	off-the-self	NA	NA	TIM

Used material properties of the pellets are shown in reference[10]. The property values are 4×10^{-4} V/K for a Seebeck coefficient, 2×10^{-5} Ω-m for an electrical resistivity, and 2.1 W/m-K for a thermal conductivity. The used electrical contact resistivity at a pellet interface is 1×10^{-9} Ω-m^2.

4.2 Optimized Pellet Geometries

Pellet height, pellet cross sectional area, and number of thermocouples were optimized. The optimization technique is not complicated but straightforward. The TE model (Eqs. (1,2), (5,6), and (9,10)) predicts generated power values under broad ranges of pellet height, pellet cross sectional area, and number of thermocouples at various source heat flows. The optimized pellet geometries are determined when the predicted power value is maximum. It should be noted that three pellet geometries were simultaneously optimized.

The optimized values of pellet geometries are shown in Table 2. It should be noted that a load resistance of 10Ω were used for the optimization.

Optimized H is found to be consistent as 3mm. It is mainly due to the fact that the power generation is strongly affected by the temperature difference across the TEG, i.e., the temperature difference between the TEG hot and cold sides.

Optimized values of A_p are seen to increase as the increase of the source heat rate, and the values range from 0.47 to 1.48 mm^2. It is mainly due to the increase of a thermal conductance as the increase of the source heat rate in order to keep the junction temperature at 200°C, which is a typical value of the junction temperatures of high power amplifier transistors.

Optimized values of N are seen to increase as the increase of the source heat rate, and the values range from 36 to 114. This interesting result can be explained similarly as the case of the optimized A_p.

Table 2 Optimized pellet geometries at various source heat flows

Case	q_{tot} (W)	H (mm)	Ap (mm^2)	N
I	5	3	0.47	36
I	10	3	0.67	52
I	15	3	0.84	63
I	20	3	0.97	74
I	25	3	1.11	83
II	5	3	0.49	38
II	10	3	0.75	56
II	15	3	0.96	75
II	20	3	1.24	91
II	25	3	1.48	114

4.3 Power Generation and Efficiency of the TEG

This section discusses generated powers (Fig. 5) and generation efficiencies (Fig. 6) associated with cases I to IV, and a measurement case at various source heat rates.

It is seen that 0.18W to 0.85W are generated with case I. The case I is an ideal case associated with optimized pellet geometries and without interfacial resistances. 0.17W to 0.48W are generated with case II. Measured values range from 0.016W to 0.39W. Generated power values of cases III and IV are similar to the measured values.

It is seen that the performance improvements even range from 200% to 1000%. Hence, it is clear that optimized pellet geometries improve power generating performance considerably. It is mainly due to the fact that optimized pellet geometries create the maximum temperature difference across the TEG and the similar electrical resistance of the TEG compared with a load resistance.

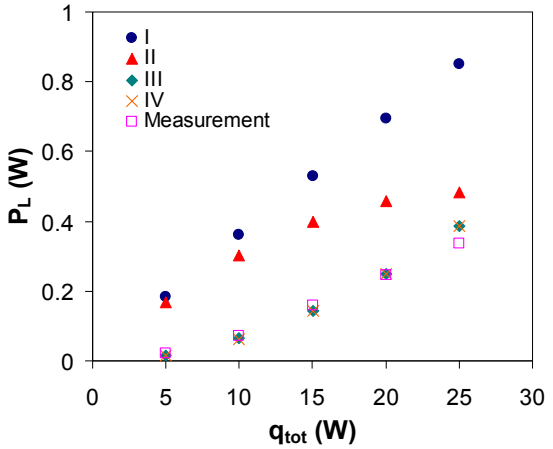

Fig. 5 Generated powers associated with cases I to IV and a measurement case as a function of source heat rates

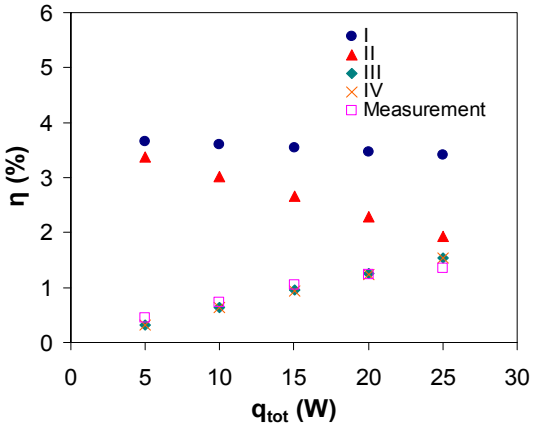

Fig. 6 Generation efficiencies associated with cases I to IV and a measurement case as a function of source heat rates

It is seen that efficiency values range from 3.4 to 3.7% for case I, 1.9 to 3.4% for case II, and 0.4 to 1.3% for the measurement. Similar to the case of the power generation, efficiency values of cases III and IV are similar to the measured values.

It is seen that optimized pellet geometries can improve the generation efficiency considerably even up to 10 times at a source heat rate of 5W. This result can be explained by the similar reasons aforementioned in the power generation analysis.

4.4 Thermal Performance of the TEG

Fig. 7 shows junction temperatures associated with cases I to IV and a measurement case as a function of source heat rates. It is seen that temperature values are consistent as 200°C for cases I and II while the values range from 41 to 111.4°C for case III, 55.4 to 182.9°C for case IV, and 60.2 to 209.9°C for the measurement. It is obvious that junction temperatures increase as the increase of the source heat rates. However, the cases associated with optimized pellet geometries show consistent temperature values. Optimized pellet geometries produce the maximum temperature difference across the TEG, and thus junction temperature values are consistent.

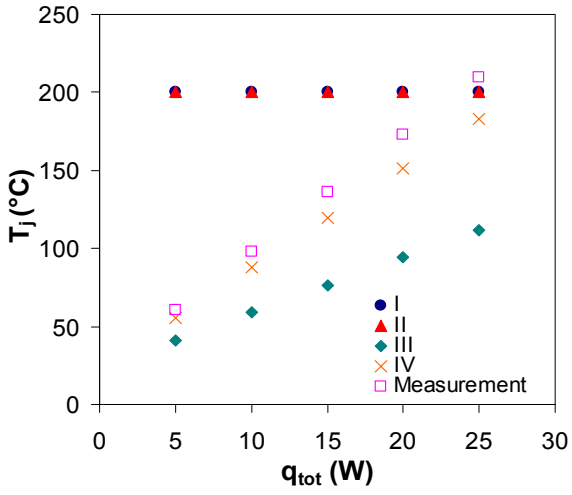

Fig. 7 Junction temperatures associated with cases I to IV and a measurement case as a function of source heat rates

5. CONCLUSIONS

This paper has reported a thermoelectric model containing thermal boundary resistances and the measurement method of the TEG performance. Then, the paper has provided optimized pellet geometries determined by using the thermoelectric model, and discussed the significant effects of the pellet geometries on the TEG performance at various source heat rates associated with two interfacial resistances.

The results show that optimized pellet geometries considerably improve both the power generation performance and the generation efficiency even up to 1000%. It is mainly due to the fact that optimized pellet geometries create the maximum temperature difference across the TEG and the similar electrical resistance of the TEG compared with a load resistance. The results show that determined temperature values associated with optimized pellet geometries are consistent despite the increase of the source heat rate. This consistency is an evidence to demonstrate that optimized pellet geometries produce the maximum temperature difference across the TEG.

Acknowledgement

This work was supported by the Pukyong National University Research Fund in 2011 (PK-2011-C-D-2011-0752).

Reference

1. D.M. Rowe (ed.), 1995, “CRC Handbook of Thermoelectrics”, CRC, Boca Raton, USA
2. G. L. Solbrekken, K. Yazawa, and A. Bar-Cohen, 2008, “Heat Driven Cooling of Portable Electronics Using Thermoelectric Technology”, IEEE Transactions on Advanced Packaging, Vol. 31, pp. 429-437.
3. K. Yazawa, G. L. Solbrekken, and A. Bar-Cohen, 2005, “Thermoelectric Powered Convective Cooling of Microprocessors”, IEEE Transactions on Advanced Packaging, Vol. 28, pp. 231 - 239.
4. J.G. Haidar and J.I. Ghojel, 2001, “Waste Heat Recovery from the Exhaust of Low-Power Diesel Engine Using Thermoelectric Generators”, Proc. of the 20th International Conference on Thermoelectrics, Beijing, China, pp. 413-417.
5. T. Kajikawa, 1997, “Status and Future Prospects on the Development of Thermoelectric Power Generation Systems Utilizing Combustion Heat from Municipal Solid Waste”, Proc. of the 16th International Conference on Thermoelectrics, Dresden, Germany, pp. 28-36.
6. A. I. Hochbaum, R. Chen, R. D. Delgado et al., 2008, “Enhanced Thermoelectric Performance of Rough Silicon Nanowires”, Nature, Vol. 451(7175), pp. 163-167.
7. K. F. Hsu, S. Loo, F. Guo et al., 2004, “Cubic AgPbmSbTe2+m: Bulk Thermoelectric Materials with High Figure of Merit”, Science, Vol. 303(5659), pp. 818-821.
8. K.J. Kim, F. Cottone, S. Goyal et al., 2010, “Energy Scavenging for Energy Efficiency in Networks and Applications”, Bell Labs Technical Journal, Vol. 15, pp. 7-30.
9. K.J. Kim, 2010, “Thermoelectric Energy Recovery from Power Amplifier Transistors”, Proc. of the 14th International Heat Transfer Conference, Washington D.C., U.S.A, 22892
10. “Product Specification Sheets”, 2009, Marlow Industries Inc.